



Spatial assessment of tap-water safety in China

Mengjie Liu^{1,2}, Nigel Graham³, Wenyu Wang¹, Renzun Zhao⁴, Yonglong Lu⁵, Menachem Elimelech^{ID 6}✉ and Wenzheng Yu^{ID 1}✉

The quality of drinking-water supplies is of fundamental importance to public health and sustainable development. Here, we provide a spatial assessment of the tap-water quality across mainland China. We examine natural and anthropogenic origins of low quality as well as its association with public health risks. By quantifying key indicators, including total organic carbon, ionic conductivity and disinfection by-products (DBPs), we find that precipitation is a crucial factor driving the change of organic matter content and ionic conductivity of tap-water, especially for arid and semi-arid regions. Although the concentration of DBPs is closely related to the organic matter content, the occurrence of highly toxic DBPs is more subject to anthropogenic factors such as economic development and pollution emission. We show that nanofiltration is an effective point-of-use treatment to reduce the adverse effects of DBPs. The present results highlight the potential health hazards associated with low-quality drinking water, suggesting that countries and regions experiencing rapid socioeconomical development might face high levels of DBP toxicity and should consider adoption of sustainability solutions.

The provision of a safe and reliable supply of drinking water is of fundamental importance to society^{1,2}. According to the 2030 Agenda for Sustainable Development, adopted by the United Nations in 2015, the sixth goal is about water quality. Conventional water treatment by coagulation–sedimentation–filtration–disinfection, the most widely used drinking-water treatment process in China, can remove 10–60% of dissolved organic matter (DOM)^{3,4}. However, disinfection by-products (DBPs) formed during the chlorine-based disinfection process are associated with adverse health outcomes (for example, bladder cancer)^{5–9} and represent a long-term public health problem with regard to drinking water¹⁰.

While several studies have evaluated the occurrence of DBPs in tap-water, these studies were conducted mainly in local regions and cities^{11–13}. Only a limited number of nationwide DBP surveys have been reported—in China¹⁴, the United Kingdom¹⁵, the United States¹⁶ and multiple European cities¹⁷—approximately a decade ago. In China, the regular monitoring of drinking-water quality is carried out by local authorities (water-supply bureaus), but this typically includes only routine parameters such as turbidity and pH. As a consequence, statistical data related to national tap-water quality, especially exposure to DBPs via tap-water and the impact of DBPs on public health, remain unclear and elusive.

China has a large land area of more than 9.6 million square kilometres, with tremendous variations in climate, topography, population density and level of economic development. Previous studies have suggested that these differences could lead to diverse compositions of DOM in soil and natural waters^{18–21}. Because natural waters serve as sources for drinking-water supply, climate-related factors and anthropogenic activities are expected to affect tap-water quality. However, there are no systematic studies on the relationship of natural factors and human activities to tap-water quality.

In this study, we conduct a comprehensive analysis of tap-water samples from 31 provinces in China (excluding Hong Kong, Macao and Taiwan) (Supplementary Fig. 1), focusing on measurements

of total organic carbon (TOC), ionic conductivity and DBPs. Our study seeks to provide answers to the following questions. (1) What is the spatial distribution of tap-water quality across China? (2) What are the correlations between natural and anthropogenic factors and tap-water quality distribution? (3) Do spatial differences in tap-water quality lead to health-risk disparity? (4) How might we deal with the health risks of poor-quality tap-water? This article discusses the water-safety issue at a large spatial scale. The results create a unique database of national tap-water quality, particularly DBPs, and provide a *prima facie* insight into the relationship between multiple factors and drinking-water safety.

Results

Impact of source water on tap-water organic content. TOC was used to evaluate the organic content of tap-water (Fig. 1a). The TOC of tap-water in different regions was greatly affected by the quality of local water sources (Supplementary Fig. 2). High TOC values in tap-water were observed in the Songhua River and Huai River basins, which have serious surface-water pollution. However, the TOC levels in the Hai River basin were relatively lower than those in surrounding areas because most cities in the Hai River basin used source water from the Changjiang (Yangtze) River basin rather than local source waters. This pattern of use is known as the South-to-North Water Diversion Project (Supplementary Fig. 3). In addition to the effect of different water sources, the TOC of tap-water was observed to increase gradually along the Changjiang River—the longest river in China (Supplementary Fig. 4). This observation can be explained partly by the intense human activity in eastern regions (Supplementary Fig. 5), which brings more pollutants from domestic wastewaters to water bodies²². In this case, pollution exceeds the self-purification capacity of the water bodies, leading to the accumulation of DOM²³.

Precipitation is a crucial natural factor that accounts for the variation of tap-water TOC by affecting the DOM in source water. It

¹State Key Laboratory of Environmental Aquatic Chemistry, Key Laboratory of Drinking Water Science and Technology, Research Center for Eco-Environmental Sciences, Chinese Academy of Sciences, Beijing, China. ²University of Chinese Academy of Sciences, Beijing, China. ³Department of Civil and Environmental Engineering, Imperial College London, London, UK. ⁴Department of Civil, Architectural and Environmental Engineering, North Carolina Agricultural and Technical State University, Greensboro, NC, USA. ⁵State Key Laboratory of Marine Environmental Science and Key Laboratory of the Ministry of Education for Coastal Wetland Ecosystems, College of the Environment and Ecology, Xiamen University, Fujian, China. ⁶Department of Chemical and Environmental Engineering, Yale University, New Haven, CT, USA. ✉e-mail: menachem.elimelech@yale.edu; wzyu@rcees.ac.cn

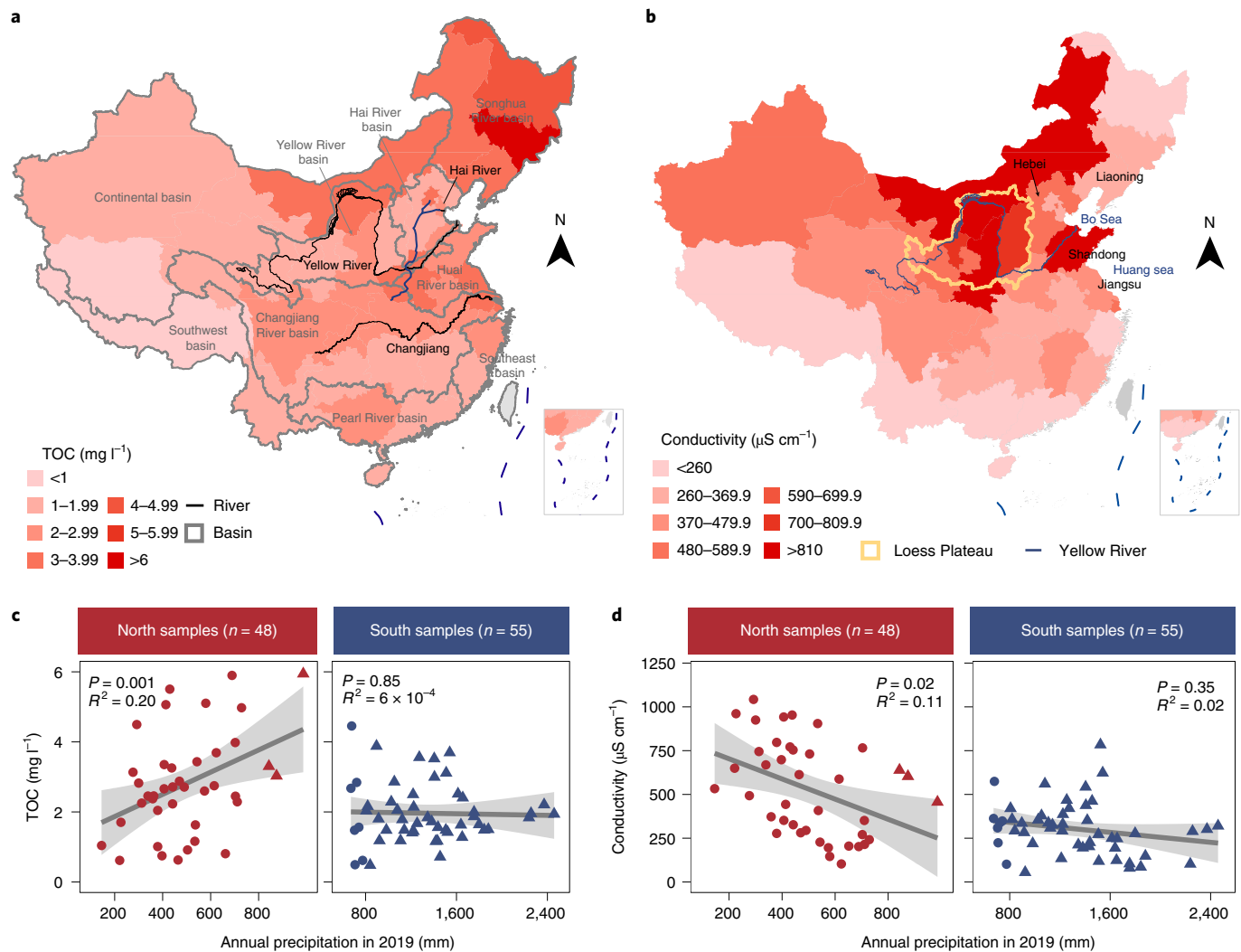


Fig. 1 | TOC and ionic conductivity of tap-water. **a**, Spatial distribution of TOC (averaged by province) in China. **b**, Spatial distribution of conductivity (averaged by province) in China. **c**, Variation of TOC with annual precipitation (in 2019), where the grey line is the linear fitting of results. The symbol shape indicates the annual precipitation (triangle: >800 mm; circle: <800 mm), and the colour indicates the location (blue: south ($n = 55$); red: north ($n = 48$))). **d**, Variation of conductivity with annual precipitation (in 2019), where the grey line is the linear fitting of results. The symbol shape indicates the annual precipitation (triangle: >800 mm, circle: <800 mm), and the colour indicates the location (blue: south ($n = 55$); red: north ($n = 48$))). Note: $810 \mu\text{S cm}^{-1}$ is equivalent to 518 mg l^{-1} total dissolved solids (TDS).

has a dual impact on DOM in natural waters: (1) atmospheric particulate matter and soil organic matter can be mobilized by precipitation and contribute DOM to run-off waters, and (2) conversely, heavy precipitation can dilute the DOM in the run-off waters. From the correlation between precipitation and the TOC of tap-water (Fig. 1b), it can be seen that TOC increases with precipitation in the northern samples but changes little with precipitation in the southern samples. The boundary between northern and southern China coincides with the 800 mm precipitation line that divides humid and sub-humid regions (Supplementary Fig. 6). For northern cities, TOC has a significant positive correlation with precipitation due to DOM mobilization from soil and atmosphere. By contrast, the dilution effect offsets the DOM mobilization in southern cities, and the TOC variation is much smaller than that in northern cities.

Soil erosion and seawater intrusion increase ionic conductivity. The variation of ionic conductivity in tap-water across China is shown in Fig. 1c. Among the eight regions, the middle Yellow River (MYR) and north coast (NC) have relatively higher conductivity

(Supplementary Fig. 7a). In addition, tap-water using the Yellow River or underground water as a source has significantly higher conductivity than others (Supplementary Fig. 7b). The Yellow River basin is known to experience intense soil erosion due to the combined impact of natural processes and human activity²⁴. The sediment load increased markedly in the middle reach of the river as it crosses the Loess Plateau²⁵, and a similar large rise in conductivity as well as Ca^{2+} concentration (for samples using the Yellow River as a water source) was evident in this region (Supplementary Fig. 8). For coastal regions, seawater intrusion and soil salinization were responsible for the high conductivity. According to the Bulletin of China Marine Disaster²⁶, seawater intrusion is serious in the coastal plain area of the Bo Sea and Huang Sea. As a result, Liaoning, Hebei, Shandong and Jiangsu provinces were found to have high conductivity. It was found that conductivity decreased with precipitation in both northern and southern China (Fig. 1d). Considering that the TOC increased with annual precipitation in northern China, we deduced a negative relationship between TOC and conductivity in this region. Previous studies have suggested

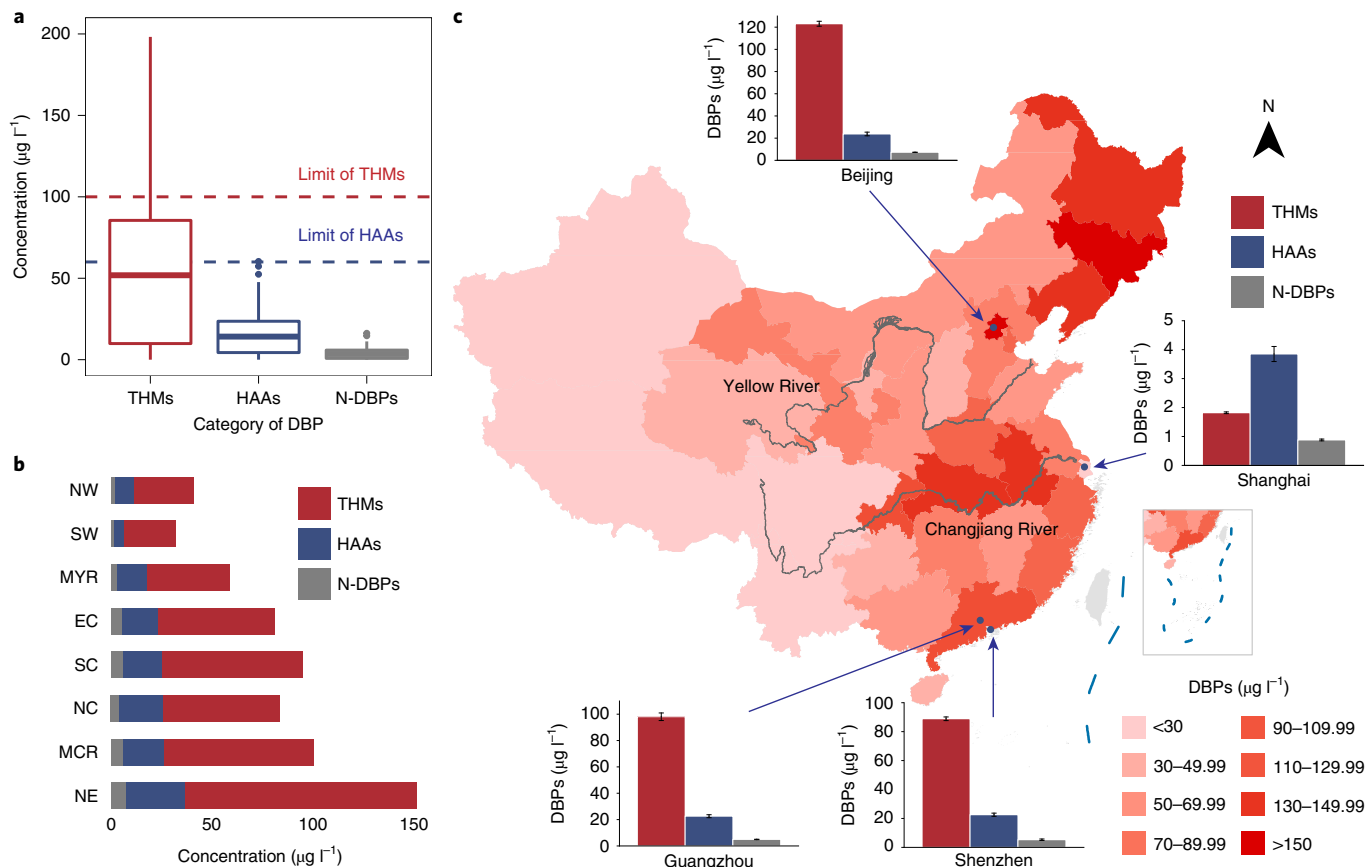


Fig. 2 | Occurrence of DBPs in tap-water samples. **a**, Box plots of three categories of DBPs (total THMs, HAAs and N-DBPs) in tap-water samples of 103 cities. The box plot displays the six-number summary of a set of data: centre line, median; box limits, upper and lower quartiles; whiskers, 1.5× interquartile range; points, outliers. Dashed lines represent the current maximum allowable levels of THMs and HAAs in drinking water in China. **b**, Average concentrations of THMs, HAAs and N-DBPs in eight economic regions: NE, NC, EC, SC, MYR, MCR, NW, SW; boundaries are shown in Supplementary Fig. 1. The colour indicates category of DBP: THMs (red), HAAs (blue) and N-DBPs (grey). **c**, Spatial distribution of DBP concentration (averaged by province) in China as a whole and in its four largest cities. Error bars represent the standard deviation (s.d.).

that when the landscape varied from desert to forest along a precipitation gradient, the root biomass and soil organic carbon content increased considerably, while the soil inorganic carbon content decreased²⁷. Our study found that this conclusion applied not only to soils, but also to tap-water in arid and semi-arid regions, indicating the connection between the soil and water environments.

Variation of DBP concentrations across China. At present, trihalomethanes (THMs) and haloacetic acids (HAAs) are the two most detected and regulated groups of DBPs, although hundreds of other DBPs have been identified and some are of greater potential toxicity²⁸. In this study, four THMs, nine HAAs and five unregulated but common nitrogen-containing DBPs (N-DBPs, including four haloacetonitrile and trichloronitromethane) were measured (Supplementary Table 1) in tap-water samples from 103 cities (Supplementary Figs. 9–11). The average total levels of THMs, HAAs and N-DBPs were $54.8 \mu\text{g l}^{-1}$, $16.1 \mu\text{g l}^{-1}$ and $3.9 \mu\text{g l}^{-1}$, respectively (Fig. 2a). We found that 88.3% and 71.8% of the samples were below the THM maximum level for drinking water in China ($100 \mu\text{g l}^{-1}$) and US EPA standard ($80 \mu\text{g l}^{-1}$), respectively, while all the samples met the requirement for HAAs. The northeast (NE) region exhibited the highest concentration of total DBPs, followed by the middle Changjiang River (MCR) and coastal regions (Fig. 2b). By contrast, the western regions (northwest (NW), southwest (SW) and MYR) had relatively lower DBP concentrations,

which is due partially to the water sources in those regions being mainly underground water with fewer DBP precursors²⁹. Among the four largest cities, Beijing, Guangzhou and Shenzhen had high concentrations of measured DBPs (Fig. 2c). Shanghai, located at the estuary of the Changjiang River, however, had a very low concentration of measured DBPs. It was reported that Shanghai is conducting a programme of upgrading its water-treatment and supply facilities. By the end of 2020, 60% of the city's water plants had adopted the combination of ozone and biological activated carbon (biofiltration) for enhanced water treatment. Ozone biofiltration has been shown to substantially reduce DBP precursors in previous studies³⁰. Advanced oxidation (for example, ozone treatment), adsorption and membrane filtration can also lower the DBP formation potential³¹. However, some of these technologies may remarkably increase the cost of water production or may bring new problems (for example, ozone by-products³²). Therefore, governments and water production utilities need to balance benefits and cost, adopting the appropriate water-quality improvement processes to reduce the health risk of drinking water.

Spatial association between DBPs and bladder cancer. High exposure to DBPs has been related to adverse health outcomes^{33–35}. Most previous studies used a case-control method focused on individuals, concluding that the case group had higher DBP exposure than the control group. In this work, we discussed this issue

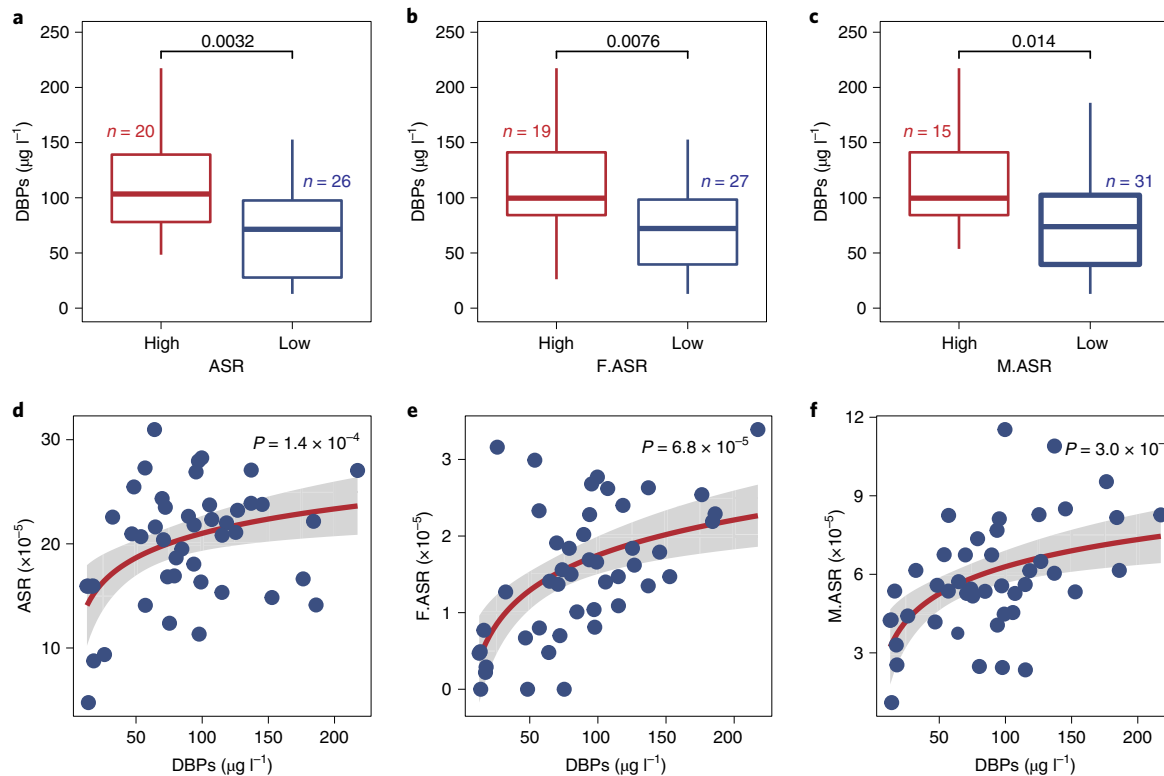


Fig. 3 | DBP association with bladder cancer. **a–c**, Comparison of DBP concentrations for cities with bladder cancer rate higher (high group) or lower (low group) than the national average for all genders (**a**), females (**b**) and males (**c**). The box plots display the six-number summary of a set of data. Results from Wilcoxon tests showed significant differences ($P < 0.05$) between the high group and the low group. Details of cancer rates in 46 cities are provided in Supplementary Table 2. **d–f**, Scatter plot showing the correlation between bladder cancer indexes and DBP concentration, where the red line is the logarithmic linear fitting of results, for all genders (**d**), females (**e**) and males (**f**). The cancer indexes: ASR, age-standardized rate; F.ASR, female ASR; M.ASR, male ASR.

from the spatial perspective. We took a closer look at 46 cities with both tumour registration information (from China's cancer registry annual report (2018)³⁶) and DBP data (measured in this study) (Supplementary Table 2), revealing that cities with a higher incidence rate for bladder cancer were characterized by higher DBP concentration in tap-water (Figs. 3a–c). Specifically, 20 cities with an age-standardized rate of bladder cancer higher than the national average had a median total concentration of measured DBPs at $103 \mu\text{g l}^{-1}$, which was significantly higher than that of the remaining 26 cities, with a median total DBP concentration of $71 \mu\text{g l}^{-1}$ ($P < 0.01$, Wilcoxon test). Linear regression further showed a log-linear relationship between the DBP concentration and the bladder cancer incidence (Figs. 3d–f). When considering the gender difference, males had a higher incidence of bladder cancer than females, but both rates were strongly associated with the concentration of DBPs. The relationships between DBPs and rectal and colon cancers were also examined (Supplementary Fig. 12); however, the statistical results are only on the verge of significance. It should be emphasized that, considering the lack of a large sample size, the result only highlights the potential link between DBPs in tap-water and bladder cancer. Other confounding variables such as tobacco consumption, diet and genetic factors are also responsible for cancer disparities³⁵. Therefore, more-detailed studies are needed to understand which populations or regions in China are more vulnerable to the health impacts of DBPs.

Spatial aggregation of cytotoxicity level of DBPs. In addition to the cancer risk, DBPs were reported to have cytotoxicity. The NC and EC regions were found to have the greatest DBP toxicity risk

(Fig. 4a). Global spatial autocorrelation (Moran's I) suggested that the calculated toxicity was spatially aggregated (Supplementary Fig. 13). Local Moran's statistics further identified local clusters and local spatial outliers of DBP toxicity (Fig. 4b). Shandong, Jiangsu, Zhejiang and Anhui provinces were the cores of high–high clusters, while Xinjiang, Tibet, Qinghai, Sichuan and Yunnan provinces were the cores of low–low clusters. Nonetheless, Shanghai (high–low point) and Chongqing (low–high point) were two spatial outliers, suggesting the calculated toxicity was significantly lower (in Shanghai) or higher (in Chongqing) than in their adjacent provinces. As discussed earlier, Shanghai had a substantially low DBP concentration due to its wide adoption of advanced treatment processes. Chongqing, one of the four municipalities directly under the central government, is the largest industrial and commercial city in southwest China. The higher level of DBP toxicity observed here indicated that anthropogenic factors also affected the water quality, which will be discussed in the subsequent section.

Link between anthropogenic factors and DBP toxicity. The preceding discussion involved TOC, conductivity, DBPs and DBP toxicity. The heat map in Supplementary Fig. 14a depicts the Pearson coefficients between each two water-quality indexes. The results showed that toxicity was highly correlated with bromine-containing DBPs (Br-DBPs) (Supplementary Fig. 14b), which is one reason for the higher toxicity observed in some coastal cities (Supplementary Fig. 15). The landward expansion of seawater or underground saltwater (directly related to seawater) along an aquifer might elevate the bromide concentration in the drinking-water source, thereby resulting in higher Br-DBP formation and greater calculated

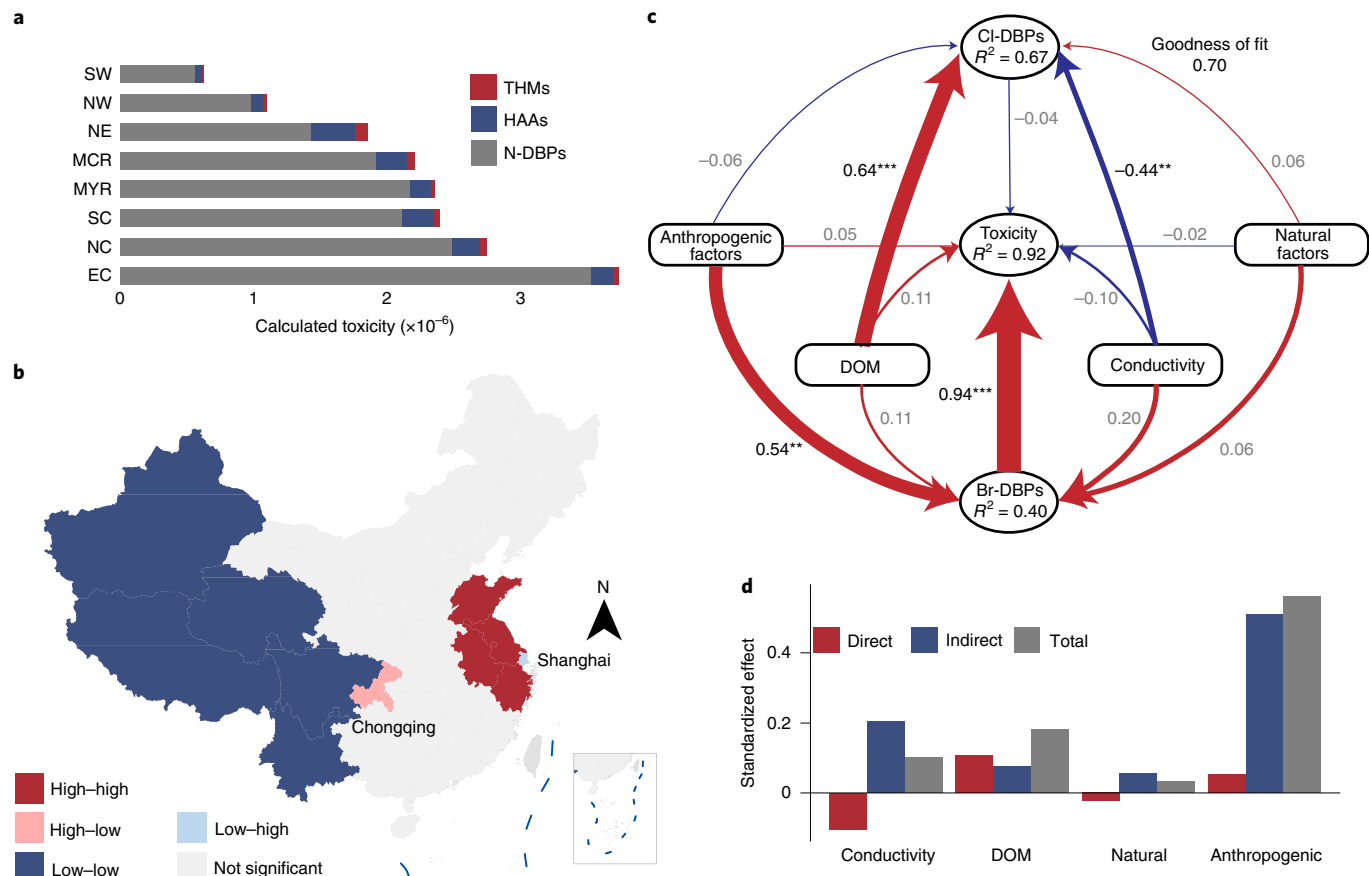


Fig. 4 | Calculated DBP cytotoxicity. **a**, Average toxicity of THMs, HAAs and N-DBPs in eight economic regions. The colour indicates category of DBP: THMs (red), HAAs (blue) and N-DBPs (grey). **b**, Local Moran cluster map of calculated DBP toxicity. Strictly speaking, the locations shown as significant on the significance and cluster maps are not the actual clusters, but rather the cores of the clusters. By contrast, in the case of spatial outliers, the locations are the actual locations of interest; **c**, PLS-PM describing the relationships between water quality and environmental factors. The composite variable DOM, natural factors, social factors, Cl-DBPs and Br-DBPs are explained in Supplementary Table 3. Larger path coefficients are shown as wider arrows, and blue and red colours indicate positive and negative effects, respectively. Path coefficients and coefficients of determination (R^2) were calculated after 999 bootstraps. Goodness of fit was 0.70. ** $P < 0.01$; *** $P < 0.001$. **d**, Standardized direct and indirect mean effects on calculated toxicity derived from the partial least-squares path models.

toxicity^{29,37}. However, we noticed Chongqing as an inland spatial outlier with significantly higher toxicity than its adjacent provinces, and thus anthropogenic factors such as the development of the city might affect the DBP toxicity in tap-water (Supplementary Fig. 15). As shown in Supplementary Table 3, significant correlation exists between calculated toxicity and several anthropogenic factors (for example, gross domestic product and waste emission).

Partial least-squares path modelling (PLS-PM) analysis was further performed to examine the complex relationships among environmental factors and water quality (Fig. 4c, Supplementary Fig. 16 and Supplementary Table 3). The DBP toxicity was more significantly affected by Br-DBPs than by chlorine-containing DBPs (Cl-DBPs). A previous study also showed that cytotoxicity was highly correlated with total organic bromine but was weakly or inversely correlated with total organic chlorine³⁷. By contrast, DOM had a stronger and more significant effect on Cl-DBPs than on Br-DBPs, which was inconsistent with the linear fit results in Supplementary Fig. 14c. Natural factors (precipitation and forest coverage rate) had weak correlation with DBP concentration and toxicity. By contrast, anthropogenic factors were significantly correlated with Br-DBPs and therefore had a strong indirect effect on DBP toxicity (Fig. 4d). This result provides one possible explanation for the association between anthropogenic factors and DBP toxicity: industrial

activities, such as the production of brominated compounds, resulted in the release of bromine to surface water³⁸, thus increasing the possibility of higher Br-DBP formation after chlorine-based disinfection as well as the associated DBP toxicity. It is unclear whether there are other pathways, for example, the difference between natural DOM and industrial DOM as well as their chlorinated DBPs, that lead to the association between anthropogenic factors and DBP toxicity. Nevertheless, our results imply that countries or regions with rapid economic development and high pollution emissions might face a higher risk of DBP toxicity exposure. Therefore, potential health hazards in drinking water caused by social development should be emphasized in future studies.

Water quality in neighbouring regions. Principal component analysis was conducted to demonstrate the relationships between samples from different regions (Fig. 5a). We observed that TOC, total fluorescence, ultraviolet (UV) absorbance at 254 nm (A_{254}) and most chlorinated DBPs are distributed along the first principal axis, while most brominated DBPs, DBP toxicity and conductivity clustered at the second principal axis, which is consistent with the results in Supplementary Fig. 14a. The samples were geographically divided into eight regions as before. NW (dark grey) and SW (light grey) samples were clustered primarily at the third quadrant,

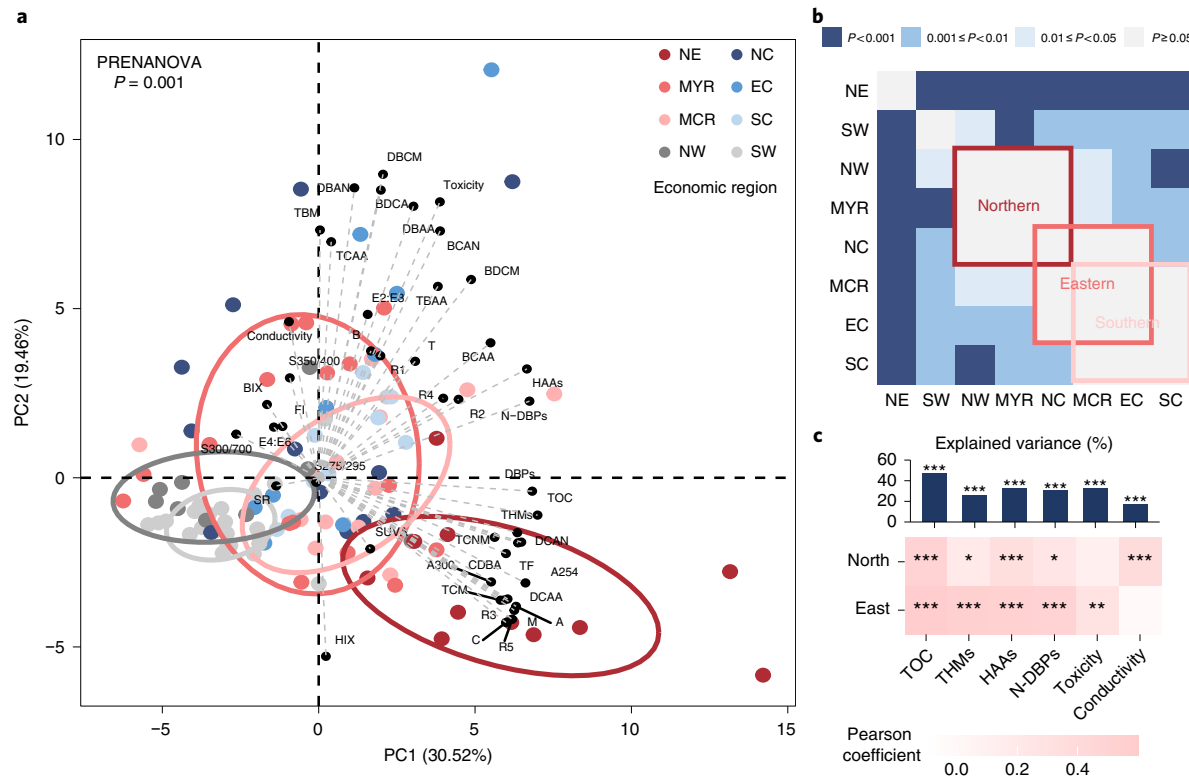


Fig. 5 | Overview of water quality and environmental factors. **a**, Principal component analysis of water-quality index. The point colour indicates the region. The indexes include TOC, A_{254} , A_{300} , specific UV absorbance (SUVA), ratio of absorbance at 250 nm to that at 365 nm (E2:E3), TF, five specific TFs (R1-R5), humification index (HIX), biological index (BIX), fluorescence index (FI) and excitation-emission matrix (EEM) peaks (A, B, C, M, T). The explanations of these water-quality indexes are summarized in Supplementary Table 4. **b**, Difference in water-quality indexes in eight regions by PERMANOVA; the colour denotes the significance level. **c**, Contribution of geographical location ('north' and 'east' directions; Methods) to water quality based on correlation and multiple regression models. The heat map shows the Pearson correlation coefficients for geographical location and water quality. * $P < 0.05$; ** $P < 0.01$; *** $P < 0.001$. The bar plot shows the total contribution of geographical location to the interpretation of water quality (obtained by multiple linear regression). The east index had a more significant correlation with all water indexes except for conductivity, suggesting that the east–west divide in water quality is more pronounced than the north–south divide.

suggesting they had relatively lower concentrations of DBPs and DOM. NE (dark red) samples, located at the positive side of the first principal axis, had a significantly higher concentration of chlorinated DBPs and DOM than other regions. Samples from coastal regions (especially for the EC) had a higher value at the second principal component, implying they had more brominated DBPs and exhibited greater DBP toxicity (Supplementary Fig. 17).

Permutational multivariate analysis of variance (PERMANOVA) further evaluated the significance of differences among the eight regions (Fig. 5b). NE and SW samples showed significant differences from samples from other regions. However, there were some linkages between the remaining six regions: (1) northern samples (NW, MYR and NC connected by the Yellow River); (2) eastern samples (NC, MCR and EC connected by the Changjiang River and the South-to-North Water Diversion Project; (3) southern samples (EC, south coast (SC) and MCR connected by water bodies in the middle and lower reaches of the Changjiang River) exhibited insignificant differences. These results imply that geographically close areas tend to exhibit similar water quality. Moreover, the correlation between water quality and geographical location (Fig. 5c) further demonstrated that the east–west divide in water quality is more pronounced than the north–south divide. The results of multiple linear regression suggested that geographical location can explain 18.9–47.0% of the variation in different water indexes. TOC had the highest explained variance, while DBP concentration is affected by

the water-treatment and disinfection parameters (disinfectant type and dosage) and thus had a lower explained variance.

Nanofiltration for improved water quality. With the deterioration of the quality of water resources and the heightened demand for high-quality drinking water, interest in using domestic water purifiers to improve tap-water quality and reduce adverse health effects has been growing rapidly in recent years³⁹. A recently published study reviewed the performances of different point-of-use strategies to decrease the DBP concentration in drinking water³⁹. Among these strategies, membrane filtration can produce water of notably higher quality with no chemical addition. In this study, we used two nanofiltration (NF) membranes with different rejection rates (NF270 and NF90) to test the improvement in water quality by NF. The results (Fig. 6a) showed that NF270 and NF90 on average decreased conductivity by 12.8% and 57.7%, respectively. For DBPs, although their molecular weights are very low (<300 Da), their hydrophobic nature resulted in a high removal rate by NF, with 66.2% and 78.2% for NF270 and NF90, respectively. The removal rates of different DBP compounds are shown in Fig. 6b. In general, molecules with more halogen atoms had a higher retention rate, and Br-DBPs were easier to remove than Cl-DBPs for DBPs with identical halogenation degrees due to their larger molecular weights³⁹. Some studies also used reverse osmosis (RO) or even multistage RO to remove DBPs^{40,41}, but one inevitable disadvantage of RO is

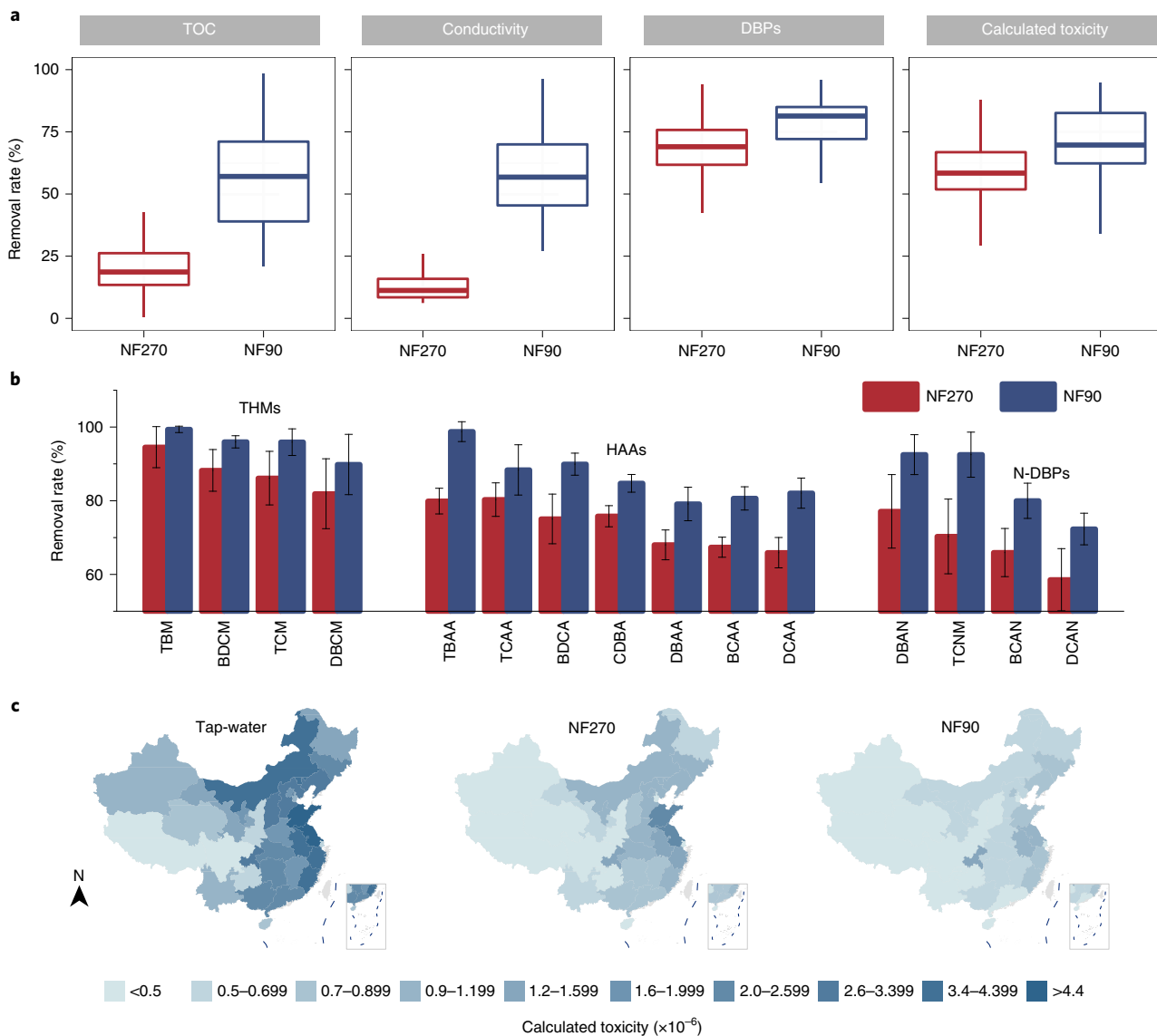


Fig. 6 | Water-quality improvement by NF. All water samples from 103 cities were treated by NF90 and NF270 membranes. **a**, Removal rate of TOC, conductivity, DBPs and calculated toxicity by two NF membranes: NF270 ('loose' NF) and NF90 ('tight' NF). The box plot displays the six-number summary of a set of data. **b**, Removal rates of different types of DBPs (THMs, HAAs and N-DBPs) by the two NF membranes. Error bars represent the s.d. Detailed information about these DBPs is given in Supplementary Table 1. **c**, Calculated toxicity of DBPs in tap-water before filtration (left) and after NF270 (middle) or NF90 (right). The calculation of calculated toxicity is shown in Methods.

the unfavourable balance between minerals and pollutants. In this study, we found that NF is sufficiently capable of removing a great portion of DBPs, thus greatly decreasing the calculated toxicity of DBPs (Fig. 6c) while leaving some minerals in place. In comparing the two NF membranes, the results suggested that using NF270 as a domestic treatment could be more effective due to its comparable DBP removal rate but nearly double water permeability compared with NF90 (Supplementary Table 5).

Discussion

This study assesses tap-water quality at a large spatial scale and discusses the driving factors as well as the adverse health outcomes. The findings revealed a significant variation of tap-water quality across China in terms of organic content, background ions and DBPs. The results further demonstrated the influence of natural and anthropogenic factors on tap-water quality and confirmed the association between DBPs and bladder cancer from the

perspective of spatial distribution. In addition, the feasibility of NF to improve water quality was tested, suggesting that NF can be used as a point-of-use treatment to reduce the health risks of DBP exposure without removing necessary minerals as RO does.

Based on the assessment of tap-water from 103 cities, the spatial distribution pattern of tap-water quality was identified. The TOC and conductivity in tap-water are closely related to water source, with precipitation playing an essential role in their spatial diversity, especially for northern China, where annual precipitation is less than 800 mm. Therefore, arid and semi-arid regions face not only water shortages but also poor drinking-water quality. The South-to-North Water Diversion Project conducted by the Chinese government provided a solution. Our results suggest that the water-diversion engineering works have not only relieved the water resource pressure on the Hai River basin but also improved the drinking-water quality in this region. The concentration of DBPs was significantly correlated with the organic content (Supplementary Fig. 14c). Therefore, the

NE region and the MCR harboured a high concentration of DBPs, while the west regions (NW and SW) faced less DBP exposure. However, the toxicity of DBPs not only was determined by the DBP concentration but also was highly affected by their composition. Key areas with significantly higher or lower DBP toxicity were identified. High toxic areas clustered at eastern coastal regions, while low toxic areas were distributed mainly at western regions. Moreover, we found that the calculated toxicity of DBPs was strongly affected by anthropogenic factors such as economic strength and pollution emission. Therefore, it is necessary to improve the coverage of advanced drinking-water treatment in economically developed cities to make up for the problems of drinking-water safety caused by economic development.

Scientists have associated DBP exposure with a variety of adverse health outcomes, including specific cancers (bladder, colon and rectal), low birth weight and miscarriages. Among these, bladder cancer has the most consistent association with DBPs in previous studies. Our study confirmed that areas with high DBPs had a significantly higher incidence of bladder cancer from a spatial distribution perspective, but the results for colon and rectal cancer were not as significant. At present, a myriad of emerging DBPs have been reported in the literature, while only a few have undergone quantification or toxicity testing⁴². Regulated DBPs (THMs and HAAs) are the most common indicators to estimate DBP exposure in epidemiological studies, and epidemiological data related to emerging DBP exposure are scarce. Therefore, it is still unclear whether emerging DBPs have other health effects on humans and whether the use of other chlorine-containing disinfectants will enhance the formation of unregulated DBPs with higher health risks.

The results in this study represent an attempt to consider drinking-water safety issues and the pattern of spatial variation in tap-water quality in terms of DBP occurrence on a national scale. However, there are still some uncertainties that deserve further investigation. First, although we tried to collect as many water samples as possible to provide accurate information on national tap-water quality, the spatial and temporal variations of DBPs in drinking water make it difficult to estimate actual human exposure. Second, we used calculated toxicity to evaluate the potential health risk of DBPs. However, calculated toxicity cannot represent the actual toxicity because of the existence of unknown DBPs^{43,44}. The recent advance in the detection of thousands of aromatic halo-DBP formulas^{45,46} as well as their transformation to aliphatic halo-DBPs⁴⁷ highlighted the potential health risk of unregulated DBPs. Therefore, the actual toxicity of DBPs in drinking water needs to be further evaluated in future studies. Third, due to the lack of records, it is challenging to conduct time-series analysis and explore the evolution of tap-water quality over time. High-resolution data (both spatial and temporal) can provide stronger evidence to identify the key factors affecting tap-water quality and important data for researchers to reveal the relationship between tap-water and human health. Therefore, it is recommended that researchers and practitioners should cooperate to perform more intensive and detailed surveys of DBPs and other contaminants at a national level, and a database of drinking-water quality should be established to provide data support for related studies.

Methods

Chemicals and materials. Methyl tert-butyl ether (MTBE) and methanol were of liquid chromatography grade and high-performance liquid chromatography grade, respectively; they were purchased from J.T. Baker. Anhydrous sodium sulfate (Na_2SO_4), sulfuric acid (H_2SO_4) and sodium bicarbonate (NaHCO_3) were obtained from Sinopharm Chemical Reagent Co. The chemical standards for DBP calibration were as follows: a THM mixture certified reference material (100 mg l^{-1} of each component in methanol, TanMo Quality Inspection Technology Co.), an HAA mixture certified reference material ($1,000\text{ mg l}^{-1}$ of each component in methanol, Sigma-Aldrich) and an N-DBP mixture certified reference material

($5,000\text{ mg l}^{-1}$ of each component in acetone, AccuStandard). Detailed information about DBPs is in Supplementary Table 1.

Sample collection and NF. Household tap-water samples were collected from 103 cities located within 31 administrative provinces and 8 regions (Supplementary Fig. 1) during March to April 2021. We collected as many samples as possible to ensure the reliability of the results. However, for some remote areas, such as northwestern China, only a small number of principal cities (that is, the capital of each province) were sampled as rural areas with low population densities typically have no centralized water-supply system. For each sampling point, two replicate water samples were collected, and the tap faucets were not equipped with a filter or other water purification unit. Before sampling, the faucet was opened for at least five minutes, the sample bottles were rinsed three times and then filled to just overflowing. All collected samples were transferred to the laboratory in ice packs as soon as possible and stored at 4°C before use.

NF tests were conducted in a dead-end filtration apparatus (Amicon 8400, Millipore) under an operational applied pressure of 4 bar. Two flat-sheet poly (piperazine-amide) membranes (NF270 and NF90, RisingSun Membrane Technology Co., Ltd.) were tested. The properties of the two membranes are given in Supplementary Table 5. To remove organic residuals, the membranes were immersed in deionized water for at least 72 hours before use. The filtrate was collected after filtering 100 ml tap-water to avoid the influence of initial adsorption.

Instrumental analysis. The chromophore and fluorescent organic substances in water samples were characterized by a UV-visible spectrophotometer (UV-2600, Shimadzu) and a three-dimensional excitation–emission matrix (EEM) spectrofluorometer (F-4600FL, Hitachi), respectively. TOC and ionic conductivity were measured using a TOC analyser (TOC-Vwp, Shimadzu) and a conductivity meter (FiveEasy Plus, Mettler Toledo). The concentration of metal ions was measured via inductively coupled plasma optical emission spectrometer (Shimadzu) after microwave digestion.

DBP extraction followed the standard methods^{48,49}. For THMs and N-DBPs, 8 g Na_2SO_4 and 4 ml MTBE were added to 20 ml water samples. After shaking for 2 min and standing for 20 min, the supernatant was transferred to a GC vial and analysed by gas chromatography (Clarus 590, PerkinElmer) with an electron capture detector (GC-ECD). For HAAs, 1 ml sulfuric acid (H_2SO_4) was added to 20 ml water samples to adjust the pH to less than 0.5. Na_2SO_4 was then added and the sample was shaken for 1 min. Subsequently, MTBE was added and the sample was shaken for 2 min. The supernatant containing HAAs was drawn out and then methylated by adding acidic methanol (containing 10 wt% H_2SO_4), followed by water-bath heating at 50°C for 2 h. Finally, 7.5 ml Na_2SO_4 (150 g l^{-1}) and 1.5 ml saturated NaHCO_3 solution were added to the methylated HAAs, and the supernatant was transferred to the GC vial for GC-ECD measurement. Each sample was prepared in duplicate. Conditions for the analyses were as follows: (1) THMs and N-DBPs, injector temperature 200°C , column temperature 35°C (holding four minutes) to 260°C ($10^\circ\text{C min}^{-1}$), detector temperature 290°C ; (2) HAAs, injector temperature 200°C , column temperature 35°C (holding for 4 min) to 65°C (2°C min^{-1}), detector temperature 290°C .

Calculation of DBP toxicity. The calculated toxicities of 18 measured DBPs (referred to as the ‘calculated toxicity’ in the main text) were calculated by summing the individual toxic potency-weighted DBP concentrations (equation (1)). The median lethal concentration(LC_{50}) values were obtained from published literature⁵⁰ and are provided in Supplementary Table 1.

$$\text{CHO cytotoxicity index} = \sum_1^n \frac{[\text{DBP}]_i}{\text{LC}_{50,i}} \quad (1)$$

Data source. The age-standardized rates for bladder, colon and rectal cancers (Supplementary Table 2) were obtained from the China cancer registry annual report (2018)⁵¹. Data concerning environmental stress factors were collected from different types of databases, including the China Statistical Yearbook, China Statistical Yearbook on Environment and others (Supplementary Table 3). The map data were downloaded from the Resource and Environment Science and Data Centre, China (<https://www.resdc.cn/Default.aspx>); detailed information is listed in Supplementary Table 6.

Relative position of sample point. The indexes ‘north’ and ‘east’ were used to describe the relative position of a sample point. For a city with latitude of x and longitude of y , the calculations of north and east were as follows:

$$\text{north} = \frac{x - x_{\min}}{x_{\max} - x_{\min}} \quad (2)$$

$$\text{east} = \frac{y - y_{\min}}{y_{\max} - y_{\min}} \quad (3)$$

The x_{\min} and x_{\max} are the latitudes of the southernmost and northernmost locations of China ($3^{\circ}51'N$ and $53^{\circ}33'N$). The y_{\min} and y_{\max} are the longitudes of the westernmost and easternmost locations of China ($73^{\circ}33'E$ and $135^{\circ}05'E$).

Data analysis. Spatial mapping was performed with ArcMap 10.6 for the 31 provinces, excluding Hong Kong, Macao and Taiwan due to sample unavailability. Data analyses were performed with the R software (4.0.5). EEM data were corrected, and the optical parameters (Supplementary Table 4) were calculated from UV absorbance and corrected EEM data via the R package (named staRdom). In addition, EEM data were divided into five regions, and the volumetric integration under the EEM within each region was calculated according to previous study⁵¹. Principal component analysis and PERMANOVA were performed by using the R package (named vegan). Function lm from the R package stats was used to conduct the linear regression. A partial Mantel test was performed to examine the correlation between location and tap-water quality using the R package (named psych). PLS-PM analysis was performed via R package (named plspm) to explore the direct and indirect relationships among environmental variables and water qualities.

Geoda (1.18.0) was used to conduct spatial autocorrelation analysis for the 31 sampled provinces⁵². Moran's I statistic is the most common indicator used for global spatial autocorrelation and is calculated as follows:

$$z_i = x_i - \bar{x} \quad (4)$$

$$S_0 = \sum_i \sum_j w_{ij} \quad (5)$$

$$I = \frac{\sum_i \sum_j w_{ij} z_i \times z_j / S_0}{\sum_i z_i^2 / n} \quad (6)$$

where \bar{x} is the mean of variable x , w_{ij} represent the elements of the spatial weight matrix and n is the number of observations.

The local Moran statistic was further performed to identify local clusters and local spatial outliers. It should be noted that the cluster maps are not the actual clusters, but the cores of a cluster. By contrast, in the case of spatial outliers, they are the actual locations of interest. More information can be found on the statistical software website⁵³.

Data availability

The water-quality data that support the findings of this study are available from the corresponding author upon reasonable request. All other data supporting the findings of this study are available within the paper and its Supplementary Information.

Received: 13 December 2021; Accepted: 21 April 2022;

Published online: 09 June 2022

References

- Prüss-Ustün, A. et al. Burden of disease from inadequate water, sanitation and hygiene in low- and middle-income settings: a retrospective analysis of data from 145 countries. *Trop. Med. Int. Health* **19**, 894–905 (2014).
- Bain, R. et al. Accounting for water quality in monitoring access to safe drinking-water as part of the Millennium Development Goals: lessons from five countries. *Bull. World Health Organ.* **90**, 228–235A (2012).
- Maqbool, T. et al. Exploring the relative changes in dissolved organic matter for assessing the water quality of full-scale drinking water treatment plants using a fluorescence ratio approach. *Water Res.* **183**, 116125 (2020).
- Li, C. et al. Tracking changes in composition and amount of dissolved organic matter throughout drinking water treatment plants by comprehensive two-dimensional gas chromatography-quadrupole mass spectrometry. *Sci. Total Environ.* **609**, 123–131 (2017).
- Sedlak, DavidL. The chlorine dilemma. *Science* **331**, 42–43 (2011).
- Shannon, M. A. et al. Science and technology for water purification in the coming decades. *Nature* **452**, 301–310 (2008).
- Li, X.-F. & Mitch, W. A. Drinking water disinfection byproducts (DBPs) and human health effects: multidisciplinary challenges and opportunities. *Environ. Sci. Technol.* **52**, 1681–1689 (2018).
- Richardson, S. D. et al. Occurrence, genotoxicity, and carcinogenicity of regulated and emerging disinfection by-products in drinking water: a review and roadmap for research. *Mutat. Res.* **636**, 178–242 (2007).
- Costet, N. et al. Water disinfection by-products and bladder cancer: is there European specificity? A pooled and meta-analysis of European case-control studies. *Occup. Environ. Med.* **68**, 379–385 (2011).
- Hao, X., Chen, G. & Yuan, Z. Water in China. *Water Res.* **169**, 115256 (2020).
- Li, Z. et al. Occurrence and distribution of disinfection byproducts in domestic wastewater effluent, tap water, and surface water during the SARS-CoV-2 pandemic in China. *Environ. Sci. Technol.* **55**, 4103–4114 (2021).
- Zhou, X. et al. Factors influencing DBPs occurrence in tap water of Jinhua Region in Zhejiang Province, China. *Ecotoxicol. Environ. Saf.* **171**, 813–822 (2019).
- Wang, C. et al. Occurrence, migration and health risk of phthalates in tap water, barreled water and bottled water in Tianjin, China. *J. Hazard. Mater.* **408**, 124891 (2021).
- Ding, H. et al. Occurrence, profiling and prioritization of halogenated disinfection by-products in drinking water of China. *Environ. Sci. Process. Impacts* **15**, 1424–1429 (2013).
- Malliarou, E., Collins, C., Graham, N. & Nieuwenhuijsen, M. J. Haloacetic acids in drinking water in the United Kingdom. *Water Res.* **39**, 2722–2730 (2005).
- Disinfection Byproducts (DBP) Information Collection Rule (ICR), United States Environmental Protection Agency, DBP ICR "Aux 1" database (2000).
- Jeong, C. H. et al. Occurrence and toxicity of disinfection byproducts in European drinking waters in relation with the HIWATE epidemiology study. *Environ. Sci. Technol.* **46**, 12120–12128 (2012).
- Ding, Y. et al. Chemodiversity of soil dissolved organic matter. *Environ. Sci. Technol.* **54**, 6174–6184 (2020).
- Zhu, J. et al. Carbon stocks and changes of dead organic matter in China's forests. *Nat. Commun.* **8**, 151 (2017).
- Jiao, N. et al. Correcting a major error in assessing organic carbon pollution in natural waters. *Sci. Adv.* **7**, eabc7318 (2021).
- Tong, Y. et al. Improvement in municipal wastewater treatment alters lake nitrogen to phosphorus ratios in populated regions. *Proc. Natl Acad. Sci. USA* **117**, 11566 (2020).
- Tong, Y. et al. Decline in Chinese lake phosphorus concentration accompanied by shift in sources since 2006. *Nat. Geosci.* **10**, 507–511 (2017).
- Fang, C. et al. Characterization of dissolved organic matter and its derived disinfection byproduct formation along the Yangtze River. *Environ. Sci. Technol.* **55**, 12326–12336 (2021).
- Ran, L., Lu, X. X. & Xin, Z. Erosion-induced massive organic carbon burial and carbon emission in the Yellow River basin, China. *Biogeosciences* **11**, 945–959 (2014).
- Wang, S. et al. Reduced sediment transport in the Yellow River due to anthropogenic changes. *Nat. Geosci.* **9**, 38–41 (2016).
- Bulletin of China Marine Disaster, Ministry of Natural Resources of the People's Republic of China, Bulletin of China Marine Disaster (2018).
- Wang, Y. et al. Profile storage of organic/inorganic carbon in soil: from forest to desert. *Sci. Total Environ.* **408**, 1925–1931 (2010).
- Bond, T., Huang, J., Templeton, M. R. & Graham, N. Occurrence and control of nitrogenous disinfection by-products in drinking water—a review. *Water Res.* **45**, 4341–4354 (2011).
- Szczyka, A. et al. Regulated and unregulated halogenated disinfection byproduct formation from chlorination of saline groundwater. *Water Res.* **122**, 633–644 (2017).
- de Vera, G. A. et al. Biodegradability of DBP precursors after drinking water ozonation. *Water Res.* **106**, 550–561 (2016).
- Chuang, Y.-H. et al. Pilot-scale comparison of microfiltration/reverse osmosis and ozone/biological activated carbon with UV/hydrogen peroxide or UV/free chlorine AOP treatment for controlling disinfection byproducts during wastewater reuse. *Water Res.* **152**, 215–225 (2019).
- Liu, X. et al. Characterization of carbonyl disinfection by-products during ozonation, chlorination, and chloramination of dissolved organic matters. *Environ. Sci. Technol.* **54**, 2218–2227 (2020).
- Wright, J. M. et al. Disinfection by-product exposures and the risk of specific cardiac birth defects. *Environ. Health Perspect.* **125**, 269–277 (2017).
- Morris, R. D. et al. Chlorination, chlorination by-products, and cancer: a meta-analysis. *Am. J. Public Health* **82**, 955–963 (1992).
- Benmarhnia, T. et al. Heterogeneity in the relationship between disinfection by-products in drinking water and cancer: a systematic review. *Int. J. Environ. Res. Public Health* **15**, 979 (2018).
- Jie, H. *China Cancer Registry Annual Report 2018*. (People's Medical Publishing House, 2018).
- Yang, Y. et al. Toxic impact of bromide and iodide on drinking water disinfected with chlorine or chloramines. *Environ. Sci. Technol.* **48**, 12362–12369 (2014).
- Liu, L. et al. Spatio-temporal variations and input patterns on the legacy and novel brominated flame retardants (BFRs) in coastal rivers of North China. *Environ. Pollut.* **283**, 117093 (2021).
- Chen, B. et al. Roles and knowledge gaps of point-of-use technologies for mitigating health risks from disinfection byproducts in tap water: a critical review. *Water Res.* **200**, 117265 (2021).

40. Wang, L., Sun, Y. & Chen, B. Rejection of haloacetic acids in water by multi-stage reverse osmosis: efficiency, mechanisms, and influencing factors. *Water Res.* **144**, 383–392 (2018).
41. Chen, B. et al. Removal of disinfection byproducts in drinking water by flexible reverse osmosis: efficiency comparison, fates, influencing factors, and mechanisms. *J. Hazard. Mater.* **401**, 123408 (2021).
42. Hebert, A. et al. Innovative method for prioritizing emerging disinfection by-products (DBPs) in drinking water on the basis of their potential impact on public health. *Water Res.* **44**, 3147–3165 (2010).
43. Ersan, M. S. et al. Chloramination of iodide-containing waters: formation of iodinated disinfection byproducts and toxicity correlation with total organic halides of treated waters. *Sci. Total Environ.* **697**, 134142 (2019).
44. Wu, Q.-Y. et al. Non-volatile disinfection byproducts are far more toxic to mammalian cells than volatile byproducts. *Water Res.* **183**, 116080 (2020).
45. Zhang, H. et al. Characterization of unknown brominated disinfection byproducts during chlorination using ultrahigh resolution mass spectrometry. *Environ. Sci. Technol.* **48**, 3112–3119 (2014).
46. Han, J., Zhang, X., Jiang, J. & Li, W. How much of the total organic halogen and developmental toxicity of chlorinated drinking water might be attributed to aromatic halogenated DBPs? *Environ. Sci. Technol.* **55**, 5906–5916 (2021).
47. Jiang, J., Han, J. & Zhang, X. Nonhalogenated aromatic DBPs in drinking water chlorination: a gap between NOM and halogenated aromatic DBPs. *Environ. Sci. Technol.* **54**, 1646–1656 (2020).
48. US Method 552.3: Determination of Haloacetic Acids and Dalapon in Drinking Water by Liquid-Liquid Microextraction, Derivatization, and Gas Chromatography with Electron Capture Detection EPA 815-B-03-002, Revision 1.0 (EPA, 2003).
49. US Method 551.1: Determination of Chlorination Disinfection Byproducts, Chlorinated Solvents, and Halogenated Pesticides/Herbicides in Drinking Water by Liquid-Liquid Extraction and Gas Chromatography With Electron-Capture Detection Revision 1.0 (EPA, 1995).
50. Lau, S. S. et al. Assessing additivity of cytotoxicity associated with disinfection byproducts in potable reuse and conventional drinking waters. *Environ. Sci. Technol.* **54**, 5729–5736 (2020).
51. Chen, W., Westerhoff, P., Leenheer, J. A. & Booksh, K. Fluorescence excitation–emission matrix regional integration to quantify spectra for dissolved organic matter. *Environ. Sci. Technol.* **37**, 5701–5710 (2003).
52. Anselin, L., Syabri, I. & Smirnov, O. Visualizing Multivariate Spatial Correlation with Dynamically Linked Windows. *New Tools for Spatial Data Analysis: Proceedings of the Specialist Meeting*, 1–20 (2002).
53. Geoda Documentation, Geoda Workbook (2022).

Acknowledgements

This work was financially supported by the Beijing Natural Science Foundation (no. JQ21032, W.Y.), Key Research and Development Plan of the Chinese Ministry of Science and Technology (no. 2019YFD1100104 and no. 2019YFC1906501, W.Y.).

Author contributions

W.Y. and M.E. originated the idea and led the research design. M.L. led the data compilation, conducted the analysis and led the write-up of the paper. M.L. and W.W. did the experiment. N.G., R.Z., Y.L., M.E. and W.Y. reviewed the paper, exchanged ideas and prepared the final version of the manuscript.

Competing interests

The authors declare no competing interests.

Additional information

Supplementary information The online version contains supplementary material available at <https://doi.org/10.1038/s41893-022-00898-5>.

Correspondence and requests for materials should be addressed to Menachem Elimelech or Wenzheng Yu.

Peer review information *Nature Sustainability* thanks Baiyang Chen, Antonio Azara, Xiangru Zhang and the other, anonymous, reviewer(s) for their contribution to the peer review of this work.

Reprints and permissions information is available at www.nature.com/reprints.

Publisher's note Springer Nature remains neutral with regard to jurisdictional claims in published maps and institutional affiliations.

© The Author(s), under exclusive licence to Springer Nature Limited 2022